Whitmarsh, R.B., Sawyer, D.S., Klaus, A., and Masson, D.G. (Eds.), 1996
*Proceedings of the Ocean Drilling Program, Scientific Results,* Vol. 149

# 32. MINERALOGICAL AND OXYGEN ISOTOPIC FEATURES OF SERPENTINITES RECOVERED FROM THE OCEAN/CONTINENT TRANSITION IN THE IBERIA ABYSSAL PLAIN[1]

Pierre Agrinier,[2] Guy Cornen,[3] and Marie-Odile Beslier[4]

**ABSTRACT**

Peridotites from the boundary between the Atlantic Ocean crust and the West Iberia continental margin (west of Portugal) were drilled during Leg 149 in Holes 897C, 897D, and 899B. These peridotites have been serpentinized intensively with more than 90% of the primary phases being essentially lizardite. No talc or antigorite were detected.

During an early episode of hydrothermal interaction (500° to 350°C), rare tremolites and chlorites formed after pyroxenes and spinel. Amphiboles are undeformed except in narrow shear zones. Serpentinization cannot be linked with this high-temperature hydrous event.

Like the serpentines drilled 100 km to the north at Hole 637A, Leg 103, the great majority of serpentines from the Leg 149 peridotites have $\delta^{18}O$ values around 10‰ and have large $\Delta^{18}O_{serpentine-magnetite}$ (12‰), which confirms that the serpentinization event occurred at low temperature (<200°C) as a consequence of the introduction of a large amount of seawater.

Calcite, which fills veins and cracks in the peridotites, precipitated from seawater at very low temperatures (19° to 13°C).

We think the lack of deep-seated serpentinization mineralogical records (antigorite and talc) that would have formed a deep low-velocity zone (shown by seismic studies at the roof of the mantle peridotites at 5 to 7 km below the top of the sediment-free basement) may be explained by retrogression of antigorite and talc to low-temperature lizardite. Another explanation is the possibility that Leg 149 peridotites do not record a high-temperature serpentinization episode because serpentinization in this deep zone was not possible. However, the complete absence of antigorite and talc in the Hole 899B peridotites (in which the low-temperature serpentines overprinted the peridotites much less intensively) and $^{18}O/^{16}O$ ratios of the lizardites do not support the first possibility unless a complete dissolution-precipitation process affected all the antigorite and the talc. The second possibility suggests that the deep low-velocity zone would not be made of serpentines.

## INTRODUCTION

The peridotite ridge and basement highs located at the ocean/continent transition of the West Iberia passive margin are composed of serpentinized peridotites. Samples were recovered during Leg 149 at Sites 897 and 899 (Shipboard Scientific Party, 1993; Sawyer, Whitmarsh, Klaus, et al., 1994; Fig. 1). Previous studies of serpentinized peridotites from the northern part of this ridge (at Hole 637A, Leg 103) show that they were emplaced during the Mesozoic continental rifting, which led to the formation of the North Atlantic Ocean (Boillot et al., 1980, 1987; Boillot, Winterer, Meyer, et al., 1987; Féraud et al., 1988; Whitmarsh et al., 1990; Schärer et al., 1995). The Hole 637A peridotites record a complex history that is characterized by a high-T, low-P ductile mylonitization followed by a multiple generation of hydrothermal alteration (Girardeau et al., 1988; Agrinier et al., 1988; Evans et al., 1988). The sequence of hydrous events occurred as follows:

1. Initially high temperature (800°-900°C) Ti- and Cr-rich pargasites formed by interaction with a metasomatic fluid or alkaline magma.
2. Hornblendes and tremolites developed after pyroxenes due to the introduction of water at lower temperatures (750°-350°C).
3. Then, at low temperature (<100°C), serpentine formed mostly because of the introduction of large amounts of cold seawater as the peridotites were being intensely fractured near the seafloor.
4. Finally, calcite precipitated from seawater at temperatures around 10°C in open fractures in the peridotites.

No clear evidence for serpentinization at high temperature was found except for the minor occurrence of talc replacing orthopyroxene. In contrast to these results, recent seismic studies of the peridotite ridge and the surroundings (Recq et al., 1991; Boillot et al, 1992; Beslier et al, 1993, Whitmarsh et al., 1993) have indicated a deep low-velocity zone ($V_p$ 7-8 km/s) dipping eastward for depths of several kilometers (5 to 7 km depth below the top of the sediment-free basement) within the lithosphere. This low-velocity horizon has been interpreted to be made of partly serpentinized mantle peridotites (Boillot et al., 1992; Beslier et al., 1993; Whitmarsh et al., 1993). Serpentinization, occurring under such conditions, would be a rather hot (about 300°C for an usual 30°/km continental geothermal gradient) and confined process, compared to the near-seafloor serpentinization described at Hole 637A, and should produce specific high pressure-high temperature minerals such as talc and antigorite. These phases are absent in the Hole 637A serpentinized ultramafic samples. This disagreement merits attention since serpentinized peridotites at depth would be a zone of weakness, leading to deformation, and potentially result in a drastically different rifting style for the peridotite ridge depending on the presence of serpentine.

In this paper, we report petrological, chemical, and $^{18}O/^{16}O$ isotopic data for serpentinized peridotite hydrous minerals from Leg 149. We compare these results to serpentinized peridotites from Leg 103 in order to constrain the pressure-temperature conditions during the hydration of the peridotites.

## SITE CHARACTERISTICS

Two of the five sites drilled during the Leg 149 encountered ultramafic rocks. These rocks were recovered from three Holes: 897C,

[1]Whitmarsh, R.B., Sawyer, D.S., Klaus, A., and Masson, D.G. (Eds.), 1996. *Proc. ODP, Sci. Results,* 149: College Station, TX (Ocean Drilling Program).
[2] Laboratoire de Géochimie des Isotopes Stables, Institut de Physique du Globe, 2 place Jussieu, F-75251 Paris cedex 05, France. piag@ccr.jussieu.fr
[3]Laboratoire de Pétrologie, Département des Sciences de la Terre, Université de Nantes, 2 rue de la Houssiniére, F-44072 Nantes cedex 03, France.
[4]Laboratoire de Géodynamique Sous-Marine, CNRS Université Pierre et Marie Curie, BP 48, F-06230 Villefranche sur Mer, France.

Reproduced online: 21 May 2004.

897D, and 899B. Holes 897C and 897D were drilled 100 m apart, in 5315 m of water. Hole 899B was drilled at about 20 km east-southeast from Site 897, at 5291 m water depth (Fig. 1)

The basement was cored over 96.2 m in Hole 897C and 152.9 m in Hole 897D. Except for the top of the basement section composed of cobbles that includes late Hauterivian to Aptian sediments and a single very thin and altered mafic occurrence, the entire sections recovered in both holes are ultramafic and extensively serpentinized. The upper part of Hole 897D has suffered an additional pervasive alteration and displays a distinct yellow to brown color. Downcore, peridotites are dominantly pale green or black, but are gray when plagioclase-bearing.

Similar lithological successions were found in both Holes 897C and 897D: beneath friable serpentinite breccias, carbonate-rich serpentinites (almost absent in Hole 897C), then brecciated serpentinites, and serpentinized peridotites including mostly harzburgite and minor lherzolite occur. In these peridotites, plagioclase and clinopyroxene are developed locally, corresponding to pods or patches of plagioclase- and olivine-bearing websterites (see Cornen et al., chapter 21, this volume; Beslier et al., this volume). Downward, banding becomes more apparent with alternating layers of dunites and harzburgites with minor lherzolitic and websteritic horizons. All rock types are coarse-grained and only the fresher samples, usually pyroxenites, display clear porphyroclastic textures (Cornen et al., chapter 21, this volume; Beslier et al., this volume).

At Site 899 the acoustic basement was cored over 180 m. The ultramafic breccia and boulders recovered were interpreted to be a mass flow deposit (Shipboard Scientific Party, 1994b; Gibson et al., this volume; Comas et al., this volume). From top to base, the sequence includes serpentinite-breccias, basaltic lavas, and sediments underlain by unbrecciated boulders of peridotites with intercalations of siltstone, unmetamorphosed basaltic lavas and microgabbros, and mafic metamorphic rocks.

Ultramafic clasts and boulders have a large range of composition from plagioclase-bearing peridotites to pyroxene- and olivine-rich peridotites. The plagioclase-bearing rocks usually contain spinel rimmed by plagioclase. Some clasts are composed of spinel and abundant contorted fibrous tremolites after pyroxenes. No plagioclase-rich websterite, nor dunite, similar to those of Site 897, have been identified. Most peridotite boulders from the lower part are fresh or weakly altered and consist of plagioclase lherzolites that grade downcore into harzburgites, locally strongly serpentinized. Some secondary chlorite and fibrous tremolite occur locally. Here again, these peridotites show coarse-grained, equant to porphyroclastic textures. No ultramafic rocks were recovered at Site 900. At this site 56 m of the basement was drilled and 27.7 m length of sheared gabbros were recovered (Shipboard Scientific Party, 1994c).

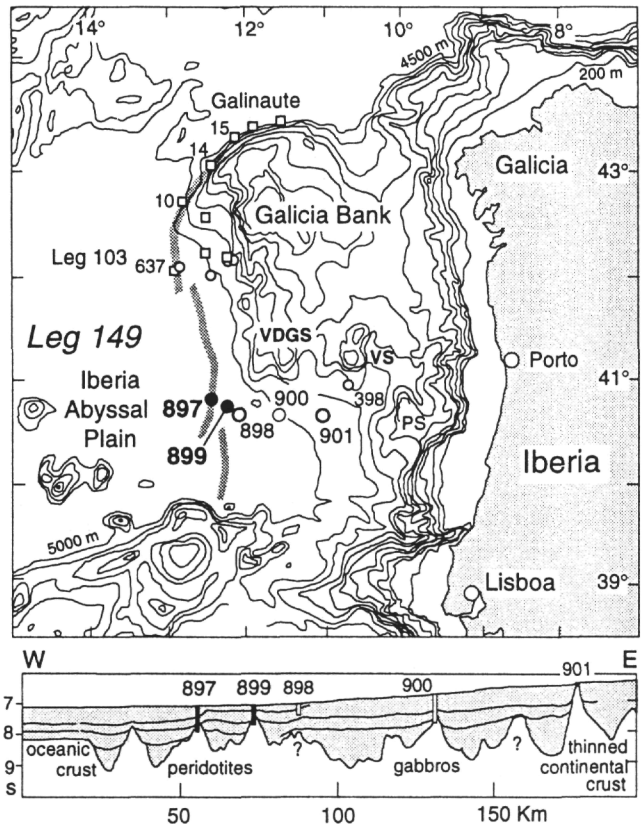


Figure 1. Top: Bathymetric map showing sites drilled at the ocean/continent boundary of the West Iberia passive margin (500-m contour intervals, 1000-m contours in bold). Sites 637 to 640 were occupied during ODP Leg 103. Sites 897 to 900 were occupied during Leg 149 (from Sawyer, Whitmarsh, Klaus, et al., 1994). Submersible sampling *(Galinaute* cruise: open squares with dive numbers) and drilling Sites of Leg 103 (circles) on the Galicia Margin and vicinity are also reported. VDGS = Vasco da Gama Seamount, VS = Vigo Seamount, PS = Porto Seamount. Bottom: Synthetic cross section of the Galicia Margin along 41°N. Depths are given in two-way traveltime (s).

## ANALYTICAL METHODS

Mineral compositions were obtained using a CAMEBAX (SX50) microprobe (Microsonde Ouest, Brest), calibrated with silicate and vanadate standards (albite, wollastonite, orthose, vanadinite) for Na, Si, Ca, K, Cl, and oxides standards for Fe, Mn, Ti, Cr, Al, and Ni. The accelerating voltage was 15 kV, the beam current 15 nA and the counting times 25 seconds (s) for Cl and Ni and 6 s for other elements. Selected representative data are listed on Tables 2 to 5.

Serpentine and magnetite were separated by hand picking, hand-held magnet, Frantz magnetic separator, and heavy liquids. After 4 hr drying at 150°C under vacuum, oxygen was extracted from silicate rocks using bromine pentafluoride at 600°C (Clayton and Mayeda, 1963) and reacted with carbon to produce $CO_2$. The $CO_2$ was extracted from carbonates by $H_3PO_4$ attack at 25.2°C for 24 hr (McCrea, 1950). $CO_2$ was introduced into a Finnigan Delta E mass spectrometer to determine the $^{18}O/^{16}O$ and $^{13}C/^{12}C$ ratios. The isotopic composition of a sample is given as $\delta_{sample} = (R_{sample}/R_{standard} - 1) \cdot 1000$ (in percent), where $R$ is the $^{18}O/^{16}O$ or $^{13}C/^{12}C$ ratio and the standard is SMOW for oxygen and PDB for carbon. Analytical errors for oxygen and carbon isotope ratios are less than 0.2‰ and 0. 1‰, respectively. During the spring to summer 1994 period, the $\delta^{18}O$ mean value of NBS 28 standard was 9.42‰ ± 0.10‰ ($\sigma$, $n$ = 9). The isotopic fractionation between two phases A and B is defined as $\Delta$ (A - B) = $\delta$A -$\delta$B ≈ 1000 ln[$\alpha$(A-B)].

## PETROGRAPHIC AND MINERALOGICAL OBSERVATIONS

A brief summary of the petrographic features follows (see also Table 1) but more details are available in Cornen et al. (chapter 21, this volume), Beslier at al. (this volume), and in the Leg 149 *Initial Reports* (Shipboard Scientific Party, 1994a, 1994b).

The peridotite samples are intensively serpentinized: more than 90% of the primary minerals are altered essentially to serpentine (lizardite, chrysotile); opaque minerals (sulfides and iron oxides), scarce chlorite, iowaite, and brucite. No talc nor antigorite were detected optically or with X-ray diffraction (XRD). Several types of serpentine were identified from the textural relationships: (1) dark or white serpentine resulting from the alteration of olivine and orthopyroxene crystals, and (2) serpentine in crosscutting veins of variable thickness

**Table 1. Nature of the analyzed serpentines and calcites.**

| Core, section, interval (cm) | Piece number | Type | Depth (mbsf) |
|---|---|---|---|
| 149-897C- | | | |
| 65R-1, 48–52 | 3B | White serpentine with calcite, from mesh serpentinized plagioclase peridotite | 669.2 ± 0.4 |
| 72R-1, 40–47 | 1E | Serpentine mesh | 726.5 ± 0.5 |
| 149-897D- | | | |
| 16R-2, 35–42 | 1C | Pale-green fibrous serpentine from vein margin in serpentinized peridotite | 743.4 ± 0.2 |
| 19R-1, 85–88 | 8E | White massive serpentine from vein | 772.4 ± 0.3 |
| 19R-4, 28–35 | 1A | White serpentine from mesh in brecciated serpentinized peridotite | 776.4 ± 0.3 |
| 19R-5, 62–69 | 3A | Tortuous white serpentine from mesh in brecciated serpentinized plagioclase peridotite | 778.9 ± 0.3 |
| 20R-2, 115–120 | 4C | Colorless serpentine from vein | 786.1 ± 0.6 |
| 23R-1, 62–68 | 5C | Serpentine mesh | 809.0 ± 0.1 |
| 24R-1, 0–5 | 1 | White massive serpentine from vein | 818.8 ± 0.2 |
| 149-899B- | | | |
| 18R-2, 18–23 | 1A | Carbonate from vein | 391.0 ± 0.2 |
| 19R-2, 0–5 | 1 | Carbonate from vein | 400.6 ± 0.3 |
| 20R-2, 100–107 | 5D | Carbonate from vein | 412.5 ± 0.4 |
| 23R-3, 121–125 | 21 | Carbonate from vein | 443.8 ± 0.3 |
| 24R-3, 87–92 | 12A | Carbonate from vein | 453.4 ± 0.3 |
| 28R-1, 118–125 | 13B | Carbonate from vein | 490.3 ± 0.8 |

Notes: Depths are the mean and standard deviation of Euler's Beta distribution (see explanations in Agrinier and Agrinier, 1994); mbsf = meters below seafloor.

(less than 1 mm to up to 20 mm), extent (1 mm to more than 10 cm), and appearance (pale-green fibrous, green, dark, white massive). The preservation of most details of the original rock texture implies that serpentinization occurred under static conditions. Pyroxenes are commonly replaced by bastite which keep their original cleavage trace. Calcite is associated with some serpentine in veins. The calcite precipitation followed the serpentine formation. The dominant vein-filling mineral changes progressively downhole from calcite to serpentine.

## Amphiboles

Amphiboles are generally uncommon in oceanic serpentinites with a few notable exceptions, including Hole 637A (Leg 103) (see also Aumento and Loubat, 1971; Roden et al., 1984; Kimball et al., 1986; Agrinier et al., 1993). Their rarity in Leg 149 ultramafics indicates that either amphiboles did not form or amphiboles that did form have been replaced by secondary phase. We are more inclined to believe in the first possibility since an exhaustive optical scan of numerous thin sections did not reveal remains of amphibole. In contrast, amphiboles are abundant in the Hole 637A serpentinites. They display a large variety of texture corresponding to a wide range of chemical composition (tremolites to pargasites) which allowed the various fluid-rock interaction stages to be described (Agrinier et al., 1988).

In the samples recovered during Leg 149 at Sites 897 and 899, different kinds of amphiboles were recorded inside mafic and ultramafic rocks. Kaersutite and Ti-richterites in unmetamorphosed alkaline lavas and microgabbros at Site 899 have a magmatic origin. Sheared gabbros recovered from the same site display pyroxene entirely replaced by chlorine-rich (up to 1.24 wt%) Ti-pargasite, by hornblende, and, at a late stage, by actinolitic hornblende and actinolite with chlorite (Fig. 2). This last association is common in the flaser gabbros of Site 900.

In the ultramafic rocks recovered during Leg 149, magmatic amphiboles are very rare. They were found only in the calcitized upper part of the Hole 897D inside some remnants of ultramafic material with unusual mineralogy. Indeed one thin section (149-897D-14R-4, 95–100 cm) displayed scarce dismembered veinlet-like ribbons with a sheared texture, set in entirely calcitized serpentinite. These ribbons are composed of clinopyroxene, Mg-ilmenite, rutile, Cr-bearing kaersutite, Ti-phlogopite, and probably former orthopyroxene, transformed to bastite. Similar mineral assemblages are known from veins inside xenoliths or peridotites with subcontinental mantle affinities. This would suggest a local metasomatism of the peridotites by alkaline melts under less severe conditions of formation than in the so-called MARID kimberlitic xenoliths (Bergman et al., 1981; Dautria et al., 1987; Lorand et al, 1990; Dawson and Smith, 1982). At Site 897, these products occur as dynamically recrystallized neoblasts, which indicates that melts infiltrated the peridotite before or during a shearing event and before the serpentinization of the orthopyroxenes.

Metamorphic amphiboles are much more abundant at Site 899 than at Site 897, although the same mineral relationships are observed at both sites. Representative amphibole compositions are reported in Table 2.

At Site 897, amphiboles are restricted to sheared plagioclase-bearing websterite where they occur around ortho- and clinopyroxene and in late brittle veins. Amphiboles are dominantly calcic, with compositions corresponding to tremolite. Amphiboles from the ultramafic rocks of Site 899 are also tremolitic and occur as (1) the main component of some clasts in the upper ultramafic breccia where they form very long, thin, and contorted white needles commonly associated to spinels (the only remnants of the primitive mineralogy), (2) syncrystallized needles with and inside large undeformed flakes of chlorite in place of primary crystals, presumably pyroxenes (Fig. 3), and (3) coarser crystals (300-500 μm) that have grown around clinopyroxenes and that constitute pockets or ribbons associated to deformation zones. In ribbons, amphiboles occur frequently as bent needles, which evidences pre- and syndeformation growths.

## Chlorite

Several types of chlorite occur in the recovered basement sections. According to the nomenclature of Hey (1954), ripidolite is the main component of some clasts and schistose boulders from Site 899. These ripidolites differ significantly from chlorite, with similar blue anomalous birefringence that locally rims spinels in ultramafic blocks recovered in the same hole. They differ also from those found in sheared amphibolites and flaser gabbros, which have a lower Fe. Cornen et al. (chapter 26, this volume) have deduced from their mineralogy that these chlorite- and sphene-bearing rocks were retrograded in the greenschist facies and that they were derived from leucogabbro or plagiogranite. A similar rock (Schärer et al., 1995), has already been sampled in situ at the top of the peridotite section in the Galicia Bank (Dive 10, Beslier et al., 1990). Other associated clasts represent

former mafic lavas inside which epidote, prehnite, and Al-chlorite have crystallized close to equilibrium. According to Liou et al. (1985), this association and the absence of pumpellyite is indicative of temperature conditions in the range of 200° to 400°C and a maximum pressure of 0.22 GPa.

Chlorite is present in the ultramafic rocks from at both Sites 897 and 899. It displays two types of occurrence: as reaction rims around spinel and as pseudomorphs after presumably clinopyroxene. In the latter case, they appear with strong birefringence color (second or third order) due to the syncrystallization of very fine needles of amphibole. Compositions are reported in Table 3. Following Hey (1954), they are clinochlore (Fig. 4A). According to Figure 4B (Laird, 1988), these chlorites are clinochlore, which plot near the 1 to 1 line corresponding to the Tschermak (TK) substitution. In ultramafic rocks, chlorites are the Al phase known to span a large range of pressure-temperature conditions from prehnite-pumpellyite facies up to upper amphibolite facies (Abbott and Raymond, 1984). At Sites 897 and 899 their relative high degree of TK substitution would indicate conditions of metamorphism corresponding to at least greenschist facies. This agrees with the stability conditions inferred by Sanford (1982) for the assemblage of chlorite-Ca amphibole occurring in reaction zones between ultramafics and varied country rocks.

## Serpentine

XRD patterns on bulk samples confirm that serpentine is mainly lizardite and accessory chrysotile. Neither antigorite nor talc was detected. Serpentine analyses are reported in the Table 4. Their composition is rather uniform in the two sites. Figure 5 discriminates clearly between aluminous-poor serpentine that replaces olivine and bastites after pyroxene, which is aluminum rich. Vein serpentines have intermediate compositions and it is suspected that the most aluminous types represent a mixture of chlorite and serpentine. One cluster of serpentine compositions displays low Al and Fe and are from chrysotile veins and their immediately adjacent serpentine from both Sites 897 and 899. Fluorine contents are low, but chlorine may be present in small concentration, up to 0.77 wt% Cl content (Fig. 6). Mesh serpentines and vein serpentines have similar Cl content. This distribution is very similar to that exemplified in Galicia Margin serpentinites by Agrinier et al. (1988).

## Iowaite and Brucite

Iowaite ($Mg_4Fe(OH)_8OCl.2\text{-}4H_2O$) was first described by Kohls and Rodda (1967) in serpentinites. It has since been found in several places, including in the Mariana and Izu-Bonin forearcs drilled during ODP Leg 125 (Helig and Swartz, 1992). During Leg 149 iowaite was identified by XRD aboard ship, mainly characterized by the peaks at 8.04 and 7.32 Å (Gibson et al., this volume). Microprobe analyses were performed on two samples that display well-developed grains. In Sample 149-897C-70R-1, 6-9 cm, iowaite rims olivine remnants in a serpentinized dunite and looks like brucite with higher birefringence (Fig. 7). Cores 897C-70R and 71R, which are composed of dunite and harzburgite, display several occurrences of this mineral. The composition reported in the Table 5, shows that iowaite contains less than 0.5% of $SiO_2$ and about 1% of alumina by weight. The mineral is a little more magnesium-rich (Mg# = 81 to 83 vs. 78) and the chlorine content, which is near 5%, appears lower than the composition (8.5%) reported by Kohls and Rodda (1967). In this sample, beside the iowaite that rims olivine $Fo_{90}$, the mesh serpentine has a "normal" composition, with Mg# close to 94 and chlorine up to 0.7%.

In another occurrence (Sample 149-897D-17R-6, 5-10 cm), a mineral with a distinct purple color appears close to brucite and calcite veins. XRD analysis revealed iowaite. In thin section, the pink-colored mineral, supposed to be iowaite, does not appear very different from serpentine between crossed polars: it composes lamellae with low birefringence and dull aspect. This material was stable under the microbeam, and analyses reveal low alumina and low FeO contents, the presence of silica in the range of 12% to 20%, chlorine up to 2.14%, and a surprisingly high Cr content (between 11% and 14% $Cr_2O_3$). Locally small spinel crystals (less than 100 µm in size) are enclosed in this pink "mineral." Serpentine from the same sample has low chlorine content (up to 0.25%). The aspect of this purple mineral and the absence of good reliability between analyses seem to correspond to a mixture of iowaite (since its characteristic X-ray peaks were detected), serpentine (which would account for the high content of silica), and an unknown Cr-bearing hydrate (which may be responsible for the color).

Brucite from the vein close to this purple mineral has a typical composition, with low FeO content (less than 0.05%) mineral and no chlorine.

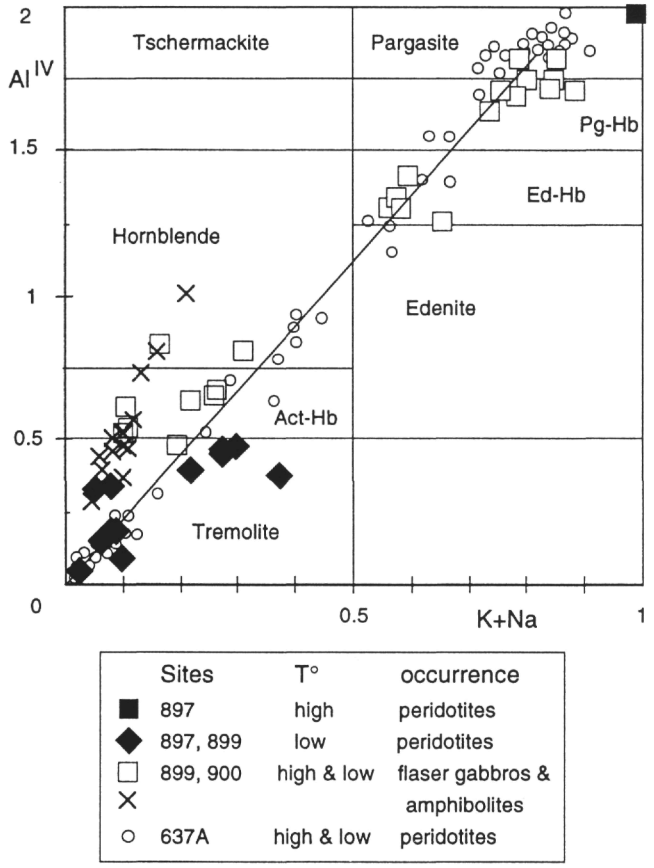


Figure 2. $Al^{IV}$ vs. K + Na diagram for calcic amphiboles. High- and low-temperature amphiboles from flaser gabbros and amphibolites of Sites 899 and 900 are reported for comparison (Cornen et al., chapter 26, this volume). Solid squares correspond to kaersutite from Sample 149-897D-14R-4, 95-100 cm. Amphibole data from serpentinized peridotites of Hole 637A (Leg 103) from Agrinier et al. (1988).

## Carbonates

Only pure calcite (Milliken and Morgan, this volume) analyses have been recorded in veins and in the carbonated mesh serpentine.

# OXYGEN AND CARBON ISOTOPE OF SERPENTINES, MAGNETITES, AND CALCITES

## Serpentine and Magnetite

Oxygen isotope results for serpentine are reported in Table 6. The oxygen isotope compositions for all the lizardite samples are strongly

**Table 2. Selected microprobe analyses of amphibole.**

| Hole: | 897C | 897D | 899B | | 899B | 899B | 899B | |
|---|---|---|---|---|---|---|---|---|
| Core, section: | 66R-4 | 14R-4 | 18R-4 | | 21R-2 | 21R-42 | 5R-2 | |
| Interval (cm): | 67–70 | 95–100 | 68–73 | | 50–55 | 82–89 | 41–46 | |
| Analysis number: | 1 | 2 | 3 | 4 | 5 | 6 | 7 | 8 |
| $SiO_2$ | 53.69 | 41.61 | 57.59 | 54.85 | 58.41 | 56.30 | 54.56 | 57.60 |
| $TiO_2$ | 0.00 | 6.83 | 0.01 | 0.00 | 0.01 | 0.03 | 0.25 | 0.12 |
| $Al_2O_3$ | 2.04 | 11.90 | 0.30 | 1.99 | 0.87 | 1.12 | 2.98 | 0.90 |
| $Cr_2O_3$ | 0.02 | 2.23 | 0.00 | 0.35 | 0.00 | 0.37 | 0.98 | 0.07 |
| FeO | 2.11 | 3.33 | 3.98 | 5.22 | 1.88 | 2.35 | 3.21 | 2.25 |
| MnO | 0.03 | 0.06 | 0.13 | 0.11 | 0.06 | 0.06 | 0.10 | 0.13 |
| NiO | 0.00 | 0.05 | 0.08 | 0.22 | 0.22 | 0.07 | 0.04 | 0.23 |
| MgO | 25.51 | 15.08 | 22.38 | 22.21 | 23.43 | 23.18 | 22.97 | 24.00 |
| CaO | 11.38 | 12.21 | 12.22 | 10.96 | 13.14 | 12.32 | 11.52 | 13.09 |
| $Na_2O$ | 0.27 | 2.73 | 0.10 | 0.20 | 0.36 | 0.30 | 1.12 | 0.24 |
| $K_2O$ | 0.04 | 1.34 | 0.00 | 0.00 | 0.04 | 0.01 | 0.00 | 0.00 |
| Cl | 0.00 | 0.00 | 0.00 | 0.04 | 0.02 | 0.10 | 0.17 | 0.00 |
| Total | 95.10 | 97.36 | 96.80 | 96.14 | 98.44 | 96.21 | 97.88 | 98.62 |
| (–O = Cl) | 0.00 | | 0.00 | –0.01 | –0.01 | –0.02 | | |
| Total | 95.10 | 97.36 | 96.80 | 96.13 | 98.43 | 96.18 | 97.88 | 98.62 |
| Si | 7.562 | 6.015 | 7.990 | 7.725 | 7.924 | 7.839 | 7.543 | 7.827 |
| $Al^{IV}$ | 0.339 | 1.985 | 0.010 | 0.275 | 0.076 | 0.161 | 0.457 | 0.145 |
| $Al^{VI}$ | 0.000 | 0.043 | 0.039 | 0.055 | 0.062 | 0.023 | 0.023 | 0.000 |
| Ti | 0.000 | 0.742 | 0.001 | 0.000 | 0.001 | 0.003 | 0.025 | 0.012 |
| Cr | 0.002 | 0.255 | 0.000 | 0.038 | 0.000 | 0.041 | 0.107 | 0.008 |
| Fe | 0.248 | 0.402 | 0.461 | 0.615 | 0.213 | 0.274 | 0.371 | 0.255 |
| Mn | 0.003 | 0.007 | 0.015 | 0.013 | 0.007 | 0.007 | 0.012 | 0.015 |
| Ni | 0.000 | 0.006 | 0.009 | 0.025 | 0.024 | 0.008 | 0.005 | 0.025 |
| Mg | 5.355 | 3.250 | 4.629 | 4.663 | 4.738 | 4.811 | 4.733 | 4.861 |
| Ca | 1.718 | 1.891 | 1.817 | 1.654 | 1.910 | 1.838 | 1.706 | 1.906 |
| $Na_B$ | 0.074 | 0.109 | 0.026 | 0.056 | 0.090 | 0.082 | 0.294 | 0.062 |
| $Na_A$ | 0.000 | 0.655 | 0.000 | 0.000 | 0.005 | 0.000 | 0.005 | 0.000 |
| K | 0.008 | 0.246 | 0.000 | 0.000 | 0.006 | 0.001 | 0.000 | 0.000 |
| Cl | 0.001 | | 0.000 | 0.009 | 0.006 | 0.024 | | |
| OH | 1.999 | 2.000 | 2.000 | 1.991 | 1.994 | 1.976 | 2.000 | 2.000 |
| Total | 17.309 | 17.606 | 16.997 | 17.119 | 17.056 | 17.0888 | 17.281 | 17.281 |
| Mg# | 95.511 | 88.822 | 90.665 | 88.139 | 95.556 | 94.489 | 92.514 | 94.735 |

Notes: Formula unit is calculated on 23 oxygen and 2 (OH, Cl) basis. Fe total is assumed as $Fe^{2+}$. Notice the high Cr content of the kaersutite from Sample 149-897D-14R-4, 95-100 cm (Analysis 2). All the analyses were performed on fibrous amphiboles except Analyses 2 and 4, which correspond to tabular crystals. Mg# = Mg • 100/(Mg + Fe).

enriched in $^{18}O$ (between 8.8‰ and 12.2‰), in comparison to the normal mantle $\delta^{18}O$ values for fresh peridotite olivine and pyroxene minerals (5‰ to 6‰; Taylor, 1968; Javoy, 1970) except for chrysotile from Sample 149-897D-16R-2, 35-42 cm, which is depleted in 18O. As oxygen is the principal constituent of silicate minerals in peridotites, such a large modification of the initial $\delta^{18}O$ requires interaction with large quantities of hydrothermal fluids during the serpentinization. High water-rock ratio conditions have been shown to be generally met in continental serpentinizing systems (Barnes and O'Neil, 1971) and oceanic serpentinized peridotites (Kimball and Gerlach, 1986; Snow and Dick, in press).

For two samples (149-897C-72R-1, 40-47 cm, and 149-897D-23R-1, 62-68 cm) the coexisting magnetite and lizardite have been measured for their $\delta^{18}O$ values. In both cases oxygen isotope fractionation, $\Delta^{18}O_{serpentine-magnetite}$, is very large (11.0‰ and 12.5‰, respectively) and is similar to the previously published values for oceanic serpentinized peridotites (Wenner and Taylor, 1973). Although the $^{18}O$ fractionation between serpentine and magnetite has not yet been calibrated vs. temperature by laboratory experiments, some natural observations and regularities have led Wenner and Taylor (1971) to propose the following "tentative" geothermometer:

$$1000 \ln[\alpha^{18}O_{serpentine-magnetite}] = 1.69 (10^6/T^2) + 1.68.$$

This calibration has been recently supported by the theoretical calculations of Zheng and Simon (1991) and Zheng (1993). Accordingly, the measured $\Delta^{18}O_{serpentine-magnetite}$ values for Sample 149-897C-72R-1, 40-47 cm, and for Sample 149-897D-23R-1, 62-68 cm, correspond to temperatures of 150°C and 120°C (±50°C), respectively. These temperatures are in the range of those determined for the lizardites (and the chrysotiles also) of the oceanic serpentinized peridotites (70° to 250°C; Wenner and Taylor, 1971; Sheppard, 1980; Bonatti et al., 1984; Hébert et al., 1990). As the associated uncertainties in these calibrations are probably considerable, these estimated temperatures mean that the serpentinization has occurred at low temperature, namely less than 200°C.

The other high $\delta^{18}O$ values of nonmagnetite paired samples are similar to the previous samples and are therefore compatible with low-temperature serpentinization processes (below 150°C) in seawater-dominated conditions. In this respect, these serpentines are similar to the serpentines from Hole 637A to the north (Agrinier et al., 1988; Evans and Girardeau, 1988). No significant difference among the various serpentine types analyzed are observed: white serpentine from veins or from the background mesh, colorless, and pale-green fibrous serpentine from vein margins, all have $\delta^{18}O$ values around 10‰. As the $\delta^{18}O$ composition of serpentine is highly sensitive to temperature change, especially at low temperature (Wenner and Taylor, 1971, 1973), this narrow range of $\delta^{18}O$ values suggests that serpentinization mostly affected these peridotites during a single (low-temperature) stage. Less equivocal than the low-temperature serpentinization conditions that can be found down to 5 km below seafloor (see estimates of the temperature gradient made from heat flux measurements; Louden and Mareschal; this volume), the high $\delta^{18}O$ values of serpentines (around 10‰) necessarily imply that serpentinization occurred under very high seawater-rock ratios (Taylor, 1977). Such seawater-rock ratio conditions are unlikely to be met deep in the crust or in the mantle. This low-temperature serpentinization very likely started when they were brought to near seafloor position.

The contrasting vein chrysotile sample (149-897D-16R-2, 35-42 cm) with a low $\delta^{18}O$ value of +3.8‰ is lower than any observed in Hole 637A and in Holes 897C, 897D, and 899B. If it results from the serpentinization of the fresh peridotite, we infer that it formed in the presence of significant amounts of fluid (high water-rock ratio) because the $\delta^{18}O$ value of this chrysotile is also strongly shifted relative

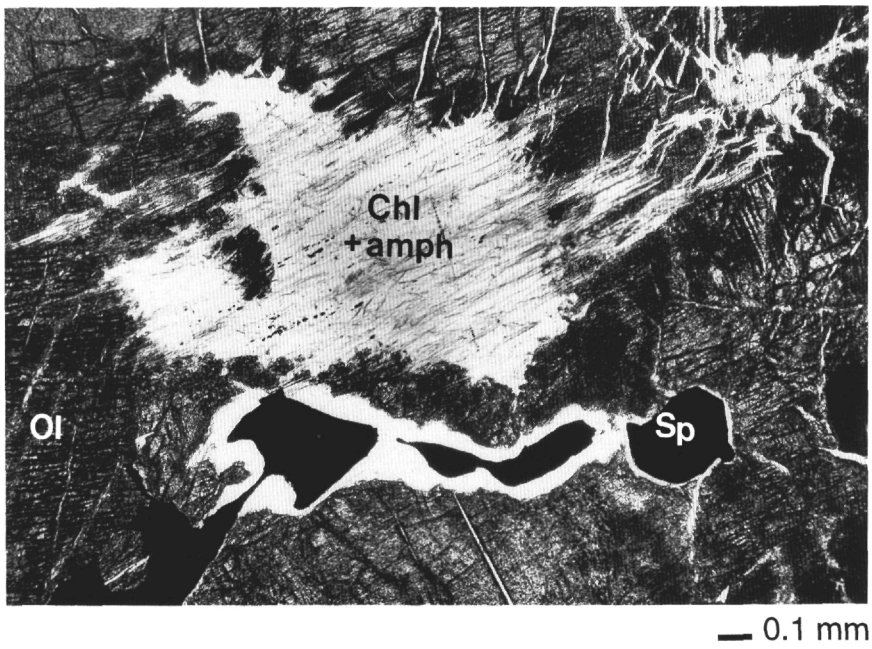


Figure 3. Photomicrograph of syncrystallized chlorite and amphibole (Chl + amph) supposed to replace orthopyroxene. Ol = olivine; Sp = spinel. The fine needles inside chlorite correspond to tremolite. Sample 149-899B-25R-2, 41-46 cm.

to its precursors (fresh olivine and orthopyroxene have $\delta^{18}O$ around 5.5‰). Since the serpentine-water oxygen isotope fractionation decreases with temperature, its low $\delta^{18}O$ value suggests that it formed at a significantly higher temperature (possibly 300°C). This chrysotile could be a remnant of the high-temperature serpentinization episode exemplified by the chlorites and the amphiboles. No other chrysotile vein sample has been recorded in Leg 149 serpentinites. The textural relationships of this sample suggest that chrysotile formed first in a vein and then was mantled by lizardite during the low-temperature serpentinization episode.

### Calcite

The carbon isotope values of calcites range from -0.7‰ to 2.4‰. They are similar to those commonly reported for seawater marine carbonates and vein carbonates from the upper oceanic crust (Javoy and Fouillac, 1979; Bonatti et al., 1980; Stakes and O'Neil, 1982). In contrast to the calcites from Hole 637A peridotites (Agrinier et al., 1988), there is no evidence for low $\delta^{13}C$ values, which would reveal some contribution from mantle carbon (Javoy and Fouillac, 1979). Calcites from veins, cracks, or from the serpentine mesh have similar $\delta^{13}C$ and $\delta^{18}O$ values. The oxygen isotope values of these calcites range from 29.6‰ to 31.1‰. This narrow range corresponds to that of low-seawater-temperature marine carbonates. Assuming the calcites formed from seawater ($\delta^{18}O$ = 0‰), calcite isotopic temperatures between 19° and 13°C can be derived (O'Neil et al., 1969). These inferred temperatures would not significantly change (less than 10°C) if these calcites formed from low-temperature $^{18}O$-depleted pore waters ($\delta^{18}O$ between 0‰ and –3‰, Lawrence et al., 1975).

## DISCUSSION AND CONCLUSION

In Leg 149 ultramafic rocks, metasomatic hydrous fluids have left mineralogical imprints that imply a polyphase hydrothermal history:

Apart from the kaersutite of Sample 149-897D-14R-4, 95-100 cm, whose growth is related to an interaction high temperature (>800°C) with a magma (see Cornen et al., this volume, chapter 21), all the amphiboles from serpentinites plot in the tremolite field, along the typical line connecting tremolite and pargasite end members. These amphiboles are different from those of the flaser gabbros and the amphibolites, which are either in pargasitic field or defined a steeper trend between the hornblende and the tremolite fields. As in Hole 637A peridotites, some of these tremolite formed by the hydration of clinopyroxene (Fig. 3), but they differ by their chemical composition (low $Al^{IV}$ content systematically, (Fig. 2) which suggests they formed under greenschist facies conditions (<500°C, Evans, 1982; Jenkins, 1983). In contrast to Hole 637A peridotites, there is no evidence of amphiboles formed at higher temperatures by interactions with hydrothermal fluids.

Although several deformation episodes affected these peridotites (Beslier et al., this volume), only tremolites in ribbons are clearly associated with a deformation event. These tremolites were formed by the penetration of hydrous fluids within high permeability zones. The other tremolites, which occur in pockets as pseudomorphs of clinopyroxene, have identical compositions and are contemporaries. The crystallization of the tremolites also predates the extensive cold complex fracturing that occurred during the serpentinization. We interpret these tremolitic amphiboles to result from the penetration of hydrothermal fluids during the uplift of the peridotites. The question of whether the hydrothermal fluid was seawater or seawater-derived fluids or neither remains equivocal.

Chlorites formed in two different situations: (1) those that syncrystallized with amphiboles as pseudomorphs of clinopyroxene and orthopyroxene (which we concluded were formed contemporaneously with amphiboles at temperatures below 500°C); and (2) those that grew after spinel. Their relative high degree of Tschermak substitution indicates conditions of metamorphism corresponding at least to greenschist facies and temperatures close to 500°C.

During this high-temperature hydrous episode, there is potential for the serpentinization of olivine since olivine is not stable below 620°C in the presence of water. Meanwhile, the case of Zabargad Island, where peridotites are completely devoid of serpentine but do contain greenschist hornblendes and actinolites (Agrinier et al., 1993), demonstrates that hydrous episodes do not necessarily imply serpentinization. However, in the case of serpentinization, according to the serpentine phase diagram (Evans et al., 1976; Caruso and Chernovsky, 1979; Chernovsky et al., 1988), antigorite should form from

**Table 3. Selected microprobe analyses of chlorite.**

| Hole: | 897C | 897C | 899B | 899B | | 899B |
|---|---|---|---|---|---|---|
| Core, section: | 67R-3 | 70R-1 | 20R-4 | 25R-2 | | 30R-1 |
| Interval (cm): | 43–50 | 6–9 | 90–96 | 41–46 | | 83–86 |
| Analysis number: | 1 | 2 | 3 | 4 | 5 | 6 |
| $SiO_2$ | 30.61 | 31.75 | 31.06 | 32.36 | 32.26 | 32.47 |
| $TiO_2$ | 0.00 | 0.08 | 0.00 | 0.16 | 0.07 | 0.00 |
| $Al_2O_3$ | 19.93 | 15.98 | 19.24 | 16.29 | 16.16 | 15.62 |
| $Cr_2O_3$ | 0.09 | 1.25 | 0.00 | 1.60 | 1.51 | 0.06 |
| FeO | 4.00 | 3.04 | 5.92 | 3.63 | 3.13 | 5.13 |
| MnO | 0.11 | 0.00 | 0.11 | 0.02 | 0.09 | 0.12 |
| NiO | 0.08 | 0.12 | 0.00 | 0.26 | 0.17 | 0.06 |
| MgO | 30.70 | 33.22 | 29.60 | 32.72 | 33.26 | 31.85 |
| CaO | 0.09 | 0.03 | 0.02 | 0.01 | 0.00 | 0.13 |
| $Na_2O$ | 0.01 | 0.00 | 0.02 | 0.08 | 0.08 | 0.06 |
| $K_2O$ | 0.01 | 0.00 | 0.41 | 0.00 | 0.00 | 0.08 |
| Cl | 0.00 | 0.00 | 0.00 | 0.02 | 0.01 | 0.06 |
| Total | 85.62 | 85.47 | 86.38 | 87.15 | 86.75 | 85.63 |
| (–O = Cl) | | | | –0.01 | –0.01 | –0.03 |
| Total | 85.62 | 85.47 | 86.38 | 87.14 | 86.74 | 85.61 |
| Si | 2.937 | 3.054 | 2.986 | 3.066 | 3.063 | 3.140 |
| $Al^{IV}$ | 1.063 | 0.946 | 1.014 | 0.934 | 0.937 | 0.860 |
| $Al^{VI}$ | 1.190 | 0.866 | 1.167 | 0.884 | 0.870 | 0.920 |
| Ti | 0.000 | 0.006 | 0.000 | 0.012 | 0.005 | 0.000 |
| Cr | 0.007 | 0.095 | 0.000 | 0.120 | 0.113 | 0.004 |
| $Fe^{2+}$ | 0.321 | 0.245 | 0.476 | 0.288 | 0.248 | 0.415 |
| Mn | 0.009 | 0.000 | 0.009 | 0.001 | 0.007 | 0.009 |
| Ni | 0.006 | 0.009 | 0.000 | 0.020 | 0.013 | 0.005 |
| Mg | 4.390 | 4.763 | 4.242 | 4.620 | 4.707 | 4.591 |
| Ca | 0.009 | 0.003 | 0.002 | 0.001 | 0.000 | 0.013 |
| Na | 0.002 | 0.000 | 0.004 | 0.015 | 0.015 | 0.012 |
| K | 0.001 | 0.000 | 0.050 | 0.000 | 0.000 | 0.010 |
| Cl | | | | 0.003 | 0.002 | 0.010 |
| Total | 9.934 | 9.986 | 9.950 | 9.964 | 9.982 | 9.989 |
| Fe# | 6.81 | 4.89 | 10.09 | 5.86 | 5.01 | 8.29 |

Note: Formula unit is calculated on 14 oxygen basis with Fe total as $Fe^{2+}$. Fe# = Fe • 100/(Fe + Mg).

olivine and talc from orthopyroxene in these conditions, while formation of chrysotile and lizardite is only possible at extremely low pressures (<2 kbar) and temperatures (<250°C).

The serpentines are predominantly lizardite, and, as shown by their $^{18}O/^{16}O$ compositions and the oxygen isotope fractionation between lizardite and magnetite, they were formed by low-temperature hydration. This hydration stage was accompanied by a complex cold fractionation associated with the emplacement of peridotites on the seafloor (Beslier et al., this volume). Apart from a single occurrence of chrysotile in a vein, which probably reflects higher temperatures of serpentinization (possibly around 300°C), we have no evidence for high-temperature (300°-400°C) serpentinization, since neither talc nor antigorite have been detected in Site 897 and 899 peridotites. Coexisting hydroxides, iowaite, and brucite confirm that the seawater-serpentinized peridotite interaction has occurred at very low temperatures and is probably still occurring. These serpentinizing conditions of the peridotites are similar to those described for the Hole 637A peridotites.

The calcites, which precipitated locally in veins and impregnate the upper parts of the serpentinized peridotites, formed at low temperature and result from circulating cold seawater within open cracks of the serpentinized peridotites. The same aspect is observed in Hole 637A peridotites.

The lack of high-temperature serpentine minerals that would form by the hydration of the Leg 149 peridotites at 5 km depth below the top of the sediment-free basement is puzzling, considering that the extent of high-temperature serpentinization of the peridotites at depth must be large—around 25% according to Christensen (1972)—to produce the decrease in $V_p$ from 8.1 to 7 km/s.

Tremolites and chlorites are too few (less than 5%) to produce such a large decrease in $V_p$. Nor can this $V_p$ decrease be due to formation of lizardite from olivine because lizardite is not stable at pressure higher than 2 kbar, according to the serpentine phase diagram (Evans et al., 1976). In the present state of the rift this lithostatic pressure is reached at 6 km below sea level. This constraint is not compatible with the serpentinization by deep penetration of cold seawater to the deep low-velocity zone (now at a depth of 10 km below sea level; Boillot et al., 1980; Whitmarsh et al, 1993) where lithostatic pressure ≈2.4 kbar) tops the upper stability limit of chrysotile and lizardite.

As mentioned above, Al-rich lizardite is stable to pressure and temperature conditions (greenschist facies) that are expected at 10 km depth. Accordingly, we may suggest that the *S* horizon is made of Al-rich lizardites formed by bastitization of orthopyroxene. Although the abundance of (bastitized) orthopyroxene is large enough, up to 20% in the Leg 149 peridotites, to account for the $V_p$ decrease, this possibility does not explain the absence of antigorite, which should form correlatively according to the serpentine phase diagram.

Finally, we think that three explanations can be made for this absence in the Leg 149 peridotites:

1. The high-temperature phases (talc, antigorite) formed at ≈10 km depth but were retrogressed to low-temperature phases (lizardite) when the peridotites reached their present seafloor position. If so, since these phases are not observed, this back-reaction process must have recrystallized the original high-temperature phases totally and readjusted the oxygen isotope compositions. This complete recrystallization is not supported by two facts. First, the Hole 899B peridotites, in which the low-temperature serpentinization overprinted the peridotites much less intensively, do not show either these of high-temperature phases. One would expect the Hole 899B peridotites to preserve at least some evidence of this presumed high-temperature serpentinization. Second, unless complete dissolution-precipitation processes affect the entire high-temperature serpentines during the back reaction, it is very difficult at low temperatures (<200°C) to reset the $\delta^{18}O$ of the serpentines from the low values compatible with the high-temperature serpentinization (like that of singular vein chrysotile) to the high values compatible with the low-temperature

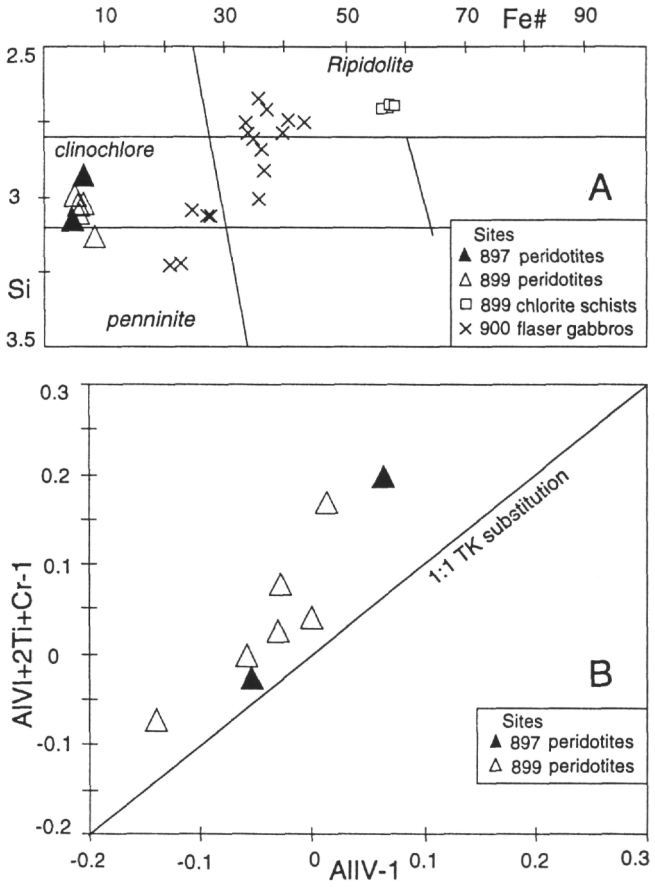


Figure 4. **A**. Chlorite of a different setting from Sites 897, 899, and 900 plotted in the grid of Hey (1954). Fe# = Fe • 100/(Fe + Mg). **B**. Chlorite from ultramafics of Sites 897 and 899 plotted in a diagram ($Al^{IV}$ + 2Ti + Cr - 1) vs. ($Al^{IV}$ - 1) (from Laird, 1988). This plot illustrates the TK substitutions with clinochlore-chamosite as the origin. Analyses plotting above the 1/1 line from the origin show dioctahedral substitution and have octahedral vacancies.

serpentinization. Experimental studies (O'Neil and Kharaka, 1976) and geological evidence (Yeh and Savin, 1976) show that the rate of oxygen exchange between clay minerals and water is extremely slow at low temperatures (<200°C) and that the antigorite to lizardite phase transformation alone is unlikely to readjust significantly the $\delta^{18}O$ of the serpentines.

2. The Leg 149 peridotites did not record a high-temperature serpentinization episode because the high-temperature phases (talc, antigorite) did not form. Most likely, the serpentinization conditions were not met at that time but were later reached when the peridotites were set near seafloor position. As said above, the Zabargad Island peridotites exemplify such a possibility. And as far as the Leg 149 peridotites are concerned in determining the nature of the deep low-velocity zone, this possibility suggests that it would not be made of serpentines.

## ACKNOWLEDGMENTS

We are indebted to J. Girardeau, C. Lecuyer, D. Teagle, A. Klaus, B. Whitmarsh, and D. Sawyer for useful comments and suggestions. The first author would like to thank Adam Klaus and Stuart R. Boyd for editing the English of this manuscript. We thank Sandra Panzolini, Agnes Michel, Michel Girard, and Jean-Jacques Bourrand for their help. This study was supported by INSU Geosciences Marines Funds.

## REFERENCES

Abbott, R.N., Jr., and Raymond, L.A., 1984. The Ashe metamorphic suite, northwest North Carolina: metamorphism and observations on geologic history. *Am. J. Sci.,* 284:350-375.

Agrinier, P., and Agrinier, B., 1994. On the knowledge of the depth of a rock sample from a drilled core. *Sci. Drill.,* 4:259-265.

Agrinier, P., Mével, C., Bosch, D., and Javoy, M., 1993. Metasomatic hydrous fluids in amphibole peridotites from Zabargad Island (Red Sea). *Earth Planet. Sci. Lett.,* 120:187-205.

Agrinier, P., Mével, C., and Girardeau, J., 1988. Hydrothermal alteration of the peridotites cored at the ocean/continent boundary of the Iberian Margin: petrologic and stable isotope evidence. *In* Boillot, G., Winterer, E.L., et al., *Proc. ODP, Sci. Results,* 103: College Station, TX (Ocean Drilling Program), 225-234.

Aumento, F., and Loubat, H., 1971. The Mid-Atlantic Ridge near 45°N. XVI. Serpentinized ultramafic intrusions. *Can. J. Earth Sci.,* 8:631-663.

Barnes, I., and O'Neil, J.R., 1971. The relationship between fluids in some fresh Alpine-type ultramafics and possible modern serpentinization, Western United States. *Bull. Geol. Soc. Am.,* 80:1947-1960.

Bergman, C., Poland, K.A., and Spera, F.J., 1981. On the origin of an amphibole-rich vein in a peridotite inclusion from the Lunar Crater volcanic field, Nevada, U.S.A. *Earth Planet. Sci. Lett.,* 56:343-361.

Beslier, M.O., Ask, M., and Boillot, G., 1993. Ocean-continent boundary in the Iberia Abyssal Plain from multichannel seismic data. *Tectonophysics,* 218:383-393.

Boillot, G., Beslier, M.O., and Comas, M., 1992. Seismic image of undercrusted serpentinite beneath a rifted margin. *Terra Nova,* 4:25-33.

Boillot, G., Grimaud, S., Mauffret, A., Mougenot, D., Kornprobst, J., Mergoil-Daniel, J., and Torrent, G., 1980. Ocean-continent boundary off the Iberian margin: a serpentinite diapir west of the Galicia Bank. *Earth Planet. Sci. Lett.,* 48:23-34.

Boillot, G., Recq, M., Winterer, E., Meyer, A.W., Applegate, J., Baltuck, M., Bergen, J.A., Comas, M.C., Davis, T.A., Dunham, K., Evans, C.A., Girardeau, J., Goldberg, D.G., Haggerty, J., Jansa, L.F., Johnson, J.A., Kasahara, J., Loreau, L.-P., Luna-Sierra, E., Moullade, M., Ogg, J., Sarti, M., Thurow, J., and Williamson, M., 1987. Tectonic denudation of the upper mantle along passive margins: a model based on drilling results (ODP Leg 103, western Galicia margin, Spain). *Tectonophysics,* 132:335-342.

Boillot, G., Winterer, E.L., Meyer, A.W., et al., 1987. *Proc. ODP, Init. Repts.,* 103: College Station, TX (Ocean Drilling Program).

Bonatti, E., Lawrence, J.R., Hamlyn, P.R., and Breger, D., 1980. Aragonite from deep sea ultramafic rocks. *Geochim. Cosmochim. Acta,* 44:1207-1214.

Bonatti, E., Lawrence, J.R., and Morandi, N., 1984. Serpentinization of ocean-floor peridotites: temperature dependence on mineralogy and boron content. *Earth Planet. Sci. Lett.,* 70:88-94.

Caruso, L.G., and Chernosky, J.V., Jr., 1979. The stability of lizardite. *Can. Mineral.,* 17:757-769.

Chernovsky, J.V., Berman, R.G., Jr., and Bryndzia, L.T., 1988. Stability, phase relations, and thermodynamic properties of chlorite and serpentine group minerals. *In* Bailey, S.W. (Ed.), *Hydrous Phyllosilicates.* Mineral. Soc. Am., Paul H. Ribbe Ser., 19:295-346.

Christensen, N.I., 1972. The abundance of serpentinites in the oceanic crust. *J. Geol.,* 80:709-719.

Clayton, R.N., and Mayeda, T.K., 1963. The use of bromine pentafluoride in the extraction of oxygen from oxides and silicates for isotopic analysis. *Geochim. Cosmochim. Acta,* 27:43-52.

Dautria, J.M, Liotard, J.M., Cabanes, N., Girod, M., and Briqueu, L., 1987. Amphibole-rich xenoliths and host alkali basalts: petrogenetic constraints and implications on the recent evolution of the upper mantle beneath Ahaggar (Central Sahara, Southern Algeria). *Contrib. Mineral. Petrol.,* 95:133-144.

Dawson, J.B., and Smith, J.V., 1982. Upper mantle amphiboles: a review. *Mineral. Mag.,* 45:35-46.

Evans, B.W., 1982. Amphiboles in metamorphosed ultramafic rocks. *In* Veblen, D.R., and Ribbe, P.H. (Eds.), *Amphiboles Review in Mineralogy.* Mineral. Soc. Am., Spec. Pap., 9B:98-113.

Evans, B.W., Johannes, W., Oterdoom, H., and Trommsdorff, V., 1976. Stability of chrysotile and antigorite in the serpentine multisystem. *Schweiz. Mineral. Petrogr. Mitt.,* 56:79-93.

Evans, C.Y., and Girardeau, J., 1988. Galicia margin peridotites: undepleted abyssal peridotites from the North Atlantic. *In* Boillot, G., Winterer, E.L., et al., *Proc. ODP, Sci. Results,* 103: College Station, TX (Ocean Drilling Program), 77-97.

Féraud, G., Girardeau, J., Beslier, M.O., and Boillot, G., 1988. Datation $^{39}Ar/^{40}Ar$ de la mise en place des péridotites bordant la marge de la Galice (Espagne). *C. R. Acad. Sci. Ser. 2,* 307:49-55.

Girardeau, J., Evans, C.A., and Beslier, M.-O., 1988. Structural analysis of plagioclase-bearing peridotites emplaced at the end of continental rifting: Hole 637A, ODP leg 103 on the Galicia Margin. *In* Boillot, G., Winterer, E.L., et al, *Proc. ODP, Sci. Results,* 103: College Station, TX (Ocean Drilling Program), 209-223.

Hébert, R., Adamson, A.C., and Komor, S.C., 1990. Metamorphic petrology of ODP Leg 109, Hole 670A serpentinized peridotites: serpentinization processes at a slow spreading ridge environment. *In* Detrick, R., Honnorez, J., Bryan, W.B., Juteau, T., et al., *Proc. ODP, Sci. Results,* 106/109: College Station, TX (Ocean Drilling Program), 103-115.

Heling, D., and Schwarz, A., 1992. Iowaite in serpentinite muds at Sites 778, 779, 780, and 784: a possible cause for the low chlorinity of pore waters. *In* Fryer, P., Pearce, J.A., Stokking, L.B., et al., *Proc. ODP, Sci. Results,* 125: College Station, TX (Ocean Drilling Program), 313-323.

Hey, M.H., 1954. A new review of the chlorites. *Mineral. Mag.,* 30:227-292.

Javoy, M., 1970. Utilisation des isotopes de l'oxygéne en magmatologie [Ph.D. thesis]. Univ, of Paris VII, Paris.

Javoy, M., and Fouillac, A.M., 1979. Stable isotope ratios in Deep Sea Drilling Project Leg 51 basalts. *In* Donnelly, T., Francheteau, J., Bryan, W., Robinson, P., Flower, M., Salisbury, M., et al., *Init. Repts. DSDP,* 51, 52, 53 (Pt. 2): Washington (U.S. Govt. Printing Office), 1153-1157.

Jenkins, D.M., 1983. Stability and composition relations of calci-amphiboles in ultramafic rocks. *Contrib. Mineral. Petrol.,* 83:375-384.

Kimball, K.L., and Gerlach, D.C., 1986. Sr isotopic constraints on hydrothermal alteration of ultramafic rocks in two oceanic fracture zones from the South Atlantic Ocean. *Earth Planet. Sci. Lett.,* 78:177-188.

Kohls, D.W., and Rodda, J.L., 1967. Iowaite, a new hydrous magnesium hydroxide-ferric oxychloride from the Precambrian of Iowa. *Am. Mineral.,* 52:1261-1271.

Laird, J., 1988. Chlorites: metamorphic petrology. *In* Bailey, S.W. (Ed.), *Hydrous Phyllosilicates.* Mineral. Soc. Am., Paul H. Ribbe Ser., 19:405-453.

Lawrence, J.R., Gieskes, J.M., and Broecker, W.S., 1975. Oxygen isotope and cation composition of DSDP pore waters and the alteration of Layer II basalts. *Earth Planet. Sci. Lett.,* 27:1-10.

Liou, J.G., Maruyama, S., and Cho, M., 1985. Phase equilibria and mineral parageneses of metabasites in low-grade metamorphism. *Mineral. Mag.,* 49:321-333.

Lorand, J.P., Vetil, J.Y., and Fabriès, J., 1990. Fe-Ti oxide assemblages of the Lherz and Freychinède amphibole rich veins (French Pyrénées). In *1st Int. Workshop on Orogenic Lherzolites and Mantle Processes:* Oxford (Blackwell Sci. Publ.), 31.

McCrea, J.M., 1950. On the isotopic chemistry of carbonates and a paleotemperature scale. *J. Chem. Phys.,* 18:849-857.

O'Neil, J.R., Clayton, R.N., and Mayeda, T.K., 1969. Oxygen isotope fractionation in divalent metal carbonates. *J. Chem. Phys.,* 51:5547-5558.

O'Neil, J.R., and Kharaka, Y.K., 1976. Hydrogen and oxygen isotope reactions between clay minerals and water. *Geochim. Cosmochim. Acta,* 40:241-246.

Recq, M., Whitmarsh, R.B., and Sibuet, J.-C., 1991. Anatomy of a lherzolitic ridge, Galicia margin. *Terra Abstr.,* 3:122.

Roden, M.K., Hart, S.R., Frey, F.A., and Melson, W.G., 1984. Sr, Nd and Pb isotopic and REE geochemistry of St-Paul's rocks: the metamorphic and metasomatic development of an alkali basalt mantle source. *Contrib. Mineral. Petrol.,* 85:376-390.

Sanford, R.S., 1982. Growth of ultramafic reaction zones in greenschist to amphibolite facies metamorphism. *Am. J. Sci.,* 182:543-616.

Sawyer, D.S., Whitmarsh, R.B., Klaus, A., et al., 1994. *Proc. ODP, Init. Repts.,* 149: College Station, TX (Ocean Drilling Program).

Schärer, U., Kornprobst, J., Beslier, M.O., Boillot, G., and Girardeau, J., 1995. Gabbro and related rock emplacement beneath rifting continental crust: U-Pb geochronological and geochemical constraints for the Galicia passive margin (Spain). *Earth Planet. Sci. Lett.,* 130:187-200.

Sheppard, S.M.F., 1980. Isotopic evidence for the origins of water during metamorphic processes in oceanic crust and ophiolite complexes. *Colloq. Int. C.N.R.S.,* 272:135-147.

Shipboard Scientific Party, 1993. ODP drills the West Iberia rifted margin. *Eos,* 74:454-455.

———, 1994a. Site 897. *In* Sawyer, D.S., Whitmarsh, R.B., Klaus, A., et al., *Proc. ODP, Init. Repts.,* 149: College Station, TX (Ocean Drilling Program), 41-113.

———, 1994b. Site 899. *In* Sawyer, D.S., Whitmarsh, R.B., Klaus, A., et al., *Proc. ODP, Init. Repts.,* 149: College Station, TX (Ocean Drilling Program), 147-209.

———, 1994c. Site 900. *In* Sawyer, D.S., Whitmarsh, R.B., Klaus, A., et al., *Proc. ODP, Init. Repts.,* 149: College Station, TX (Ocean Drilling Program), 211-262.

Snow, J.E., and Dick, H., in press. The seafloor alteration of abyssal peridotites: pervasive Mg depletion during submarine weathering. *Geochim. Cosmochim. Acta.*

Spear, F.S., 1981. An experimental study of hornblende stability and compositional variability in amphibolite. *Am. J. Sci.,* 281:697-734.

Stakes, D.S., and O'Neil, J.R., 1982. Mineralogy and stable isotope geochemistry of hydrothermally altered oceanic rocks. *Earth Planet. Sci. Lett.,* 57:285-304.

Taylor, H.P., Jr., 1968. The oxygen isotope geochemistry of igneous rocks. *Contrib. Mineral. Petrol.,* 19:1-71.

———, 1977. Water/rock interactions and the origin of $H_2O$ in granitic batholiths. *J. Geol. Soc. London,* 133:509-558.

Velde, B., 1973. Phase equilibria in the system $MgO-Al_2O_3-SiO_2-H_2O$: chlorites and associated minerals. *Mineral. Mag.,* 39:293—312.

Wenner, D.B., and Taylor, H.P., Jr., 1971. Temperatures of serpentinization of ultramafic rocks based on $^{16}O/^{18}O$ fractionation between coexisting serpentine and magnetite. *Contrib. Mineral. Petrol.,* 32:165-185.

———, 1973. Oxygen and hydrogen isotope studies of the serpentinization of ultramafic rocks in oceanic environments and continental ophiolite complexes. *Am. J. Sci.,* 273:207-239.

Whitmarsh, R.B., Miles, P.R., and Mauffret, A., 1990. The ocean-continent boundary off the western continental margin of Iberia, I. Crustal structure at 40°30'N. *Geophys. J. Int.,* 103:509-531.

Whitmarsh, R.B., Pinheiro, L.M., Miles, P.R., Recq, M., and Sibuet, J.C., 1993. Thin crust at the western Iberia ocean-continent transition and ophiolites. *Tectonics,* 12:1230-1239.

Yeh, H., and Savin, S.M., 1976. The extent of oxygen isotope exchange between clay minerals and sea water. *Geochim. Cosmochim. Acta,* 40:743-748.

Zheng, Y.-F., 1993. Calculation of oxygen isotope fractionation in hydroxyl-bearing silicates. *Earth Planet. Sci. Lett.,* 120:247-263.

Zheng, Y.-F., and Simon, K., 1991. Oxygen isotope fractionation in hematite and magnetite: a theoretical calculation and application to geothermometry of metamorphic iron-formations. *Eur. J. Mineral.,* 3:877-886.

**Date of initial receipt: 17 January 1995**
**Date of acceptance: 3 November 1995**
**Ms 149SR-223**

**Table 4. Selected analyses of serpentine.**

| Hole: | 897C | 897D | 897D | | | | 897D | 897D | | 897D | |
|---|---|---|---|---|---|---|---|---|---|---|---|
| Core, section: | 70R-1 | 16R-1 | 16R-2 | | | | 17R-6 | 19R-5 | | 20R-2 | |
| Interval (cm): | 6–9 | 33–38 | 35–42 | | | | 5–10 | 62–69 | | 115–120 | |
| Sample type: | MS | B | MS | B | ChV | V | MS | MS | B | B | V |
| $SiO_2$ | 36.98 | 41.91 | 44.95 | 38.80 | 43.73 | 41.19 | 39.91 | 38.69 | 38.03 | 37.96 | 37.57 |
| $TiO_2$ | 0.01 | 0.11 | 0.00 | 0.08 | 0.03 | 0.00 | 0.00 | 0.00 | 0.06 | 0.07 | 0.00 |
| $Al_2O_3$ | 0.07 | 3.47 | 0.20 | 2.08 | 0.51 | 2.98 | 0.27 | 0.18 | 1.47 | 5.61 | 3.47 |
| $Cr_2O_3$ | 0.00 | 0.74 | 0.00 | 0.99 | 0.00 | 0.00 | 0.20 | 0.01 | 0.67 | 0.05 | 0.02 |
| FeO | 3.95 | 4.63 | 3.67 | 5.70 | 1.94 | 2.20 | 3.89 | 5.32 | 6.05 | 3.09 | 1.85 |
| MnO | 0.04 | 0.10 | 0.01 | 0.17 | 0.14 | 0.08 | 0.10 | 0.00 | 0.19 | 0.04 | 0.11 |
| NiO | 0.07 | 0.08 | 0.23 | 0.25 | 0.08 | 0.09 | 0.13 | 0.23 | 0.00 | 0.00 | 0.00 |
| MgO | 35.78 | 34.64 | 35.72 | 34.50 | 39.50 | 39.32 | 38.51 | 37.65 | 36.39 | 37.80 | 39.55 |
| CaO | 0.02 | 0.27 | 0.15 | 0.10 | 0.00 | 0.04 | 0.01 | 0.03 | 0.01 | 0.00 | 0.13 |
| $Na_2O$ | 0.03 | 0.01 | 0.03 | 0.04 | 0.04 | 0.06 | 0.03 | 0.05 | 0.02 | 0.01 | 0.00 |
| $K_2O$ | 0.00 | 0.00 | 0.06 | 0.00 | 0.00 | 0.00 | 0.00 | 0.00 | 0.01 | 0.00 | 0.00 |
| Total | 76.95 | 85.97 | 85.02 | 82.71 | 85.97 | 85.95 | 83.03 | 82.15 | 82.89 | 84.64 | 82.69 |
| Cl | 0.67 | | 0.03 | 0.45 | 0.04 | 0.00 | 0.11 | 0.09 | 0.15 | 0.03 | 0.77 |
| F | 0.00 | | 0.00 | 0.00 | 0.01 | 0.00 | 0.02 | 0.00 | 0.00 | 0.00 | 0.02 |
| (–O = F, Cl) | –0.30 | | –0.01 | –0.20 | –0.02 | 0.00 | –0.07 | –0.04 | –0.07 | –0.01 | –0.37 |
| Total | 77.32 | 85.97 | 85.04 | 82.95 | 85.99 | 85.95 | 83.09 | 82.20 | 82.97 | 84.65 | 83.12 |
| Si | 1.953 | 1.970 | 2.119 | 1.918 | 2.041 | 1.938 | 1.953 | 1.927 | 1.881 | 1.817 | 1.843 |
| Ti | 0.000 | 0.004 | 0.000 | 0.003 | 0.001 | 0.000 | 0.000 | 0.000 | 0.002 | 0.003 | 0.000 |
| Cr | 0.000 | 0.028 | 0.000 | 0.039 | 0.000 | 0.000 | 0.008 | 0.000 | 0.026 | 0.002 | 0.001 |
| $Fe^{3+}$ | 0.175 | 0.182 | 0.145 | 0.235 | 0.075 | 0.086 | 0.159 | 0.221 | 0.250 | 0.124 | 0.076 |
| Al | 0.005 | 0.192 | 0.011 | 0.121 | 0.028 | 0.164 | 0.015 | 0.010 | 0.086 | 0.317 | 0.201 |
| Mn | 0.002 | 0.004 | 0.000 | 0.007 | 0.006 | 0.003 | 0.004 | 0.000 | 0.008 | 0.002 | 0.000 |
| Ni | 0.003 | 0.003 | 0.009 | 0.010 | 0.003 | 0.003 | 0.005 | 0.000 | 0.000 | 0.000 | 0.000 |
| Mg | 2.817 | 2.427 | 2.509 | 2.542 | 2.749 | 2.738 | 2.809 | 2.795 | 2.682 | 2.696 | 2.892 |
| Ca | 0.001 | 0.014 | 0.008 | 0.005 | 0.000 | 0.002 | 0.001 | 0.001 | 0.000 | 0.000 | 0.007 |
| Na | 0.003 | 0.001 | 0.003 | 0.004 | 0.004 | 0.005 | 0.002 | 0.005 | 0.002 | 0.001 | 0.000 |
| K | 0.000 | 0.000 | 0.003 | 0.000 | 0.000 | 0.000 | 0.000 | 0.000 | 0.001 | 0.000 | 0.000 |
| Total | 4.958 | 4.825 | 4.806 | 4.883 | 4.906 | 4.939 | 4.956 | 4.959 | 4.937 | 4.960 | 5.018 |
| Cl | 0.060 | 0.000 | 0.002 | 0.038 | 0.003 | 0.000 | 0.009 | 0.008 | 0.013 | 0.003 | 0.064 |
| F | 0.000 | | 0.000 | 0.000 | 0.001 | 0.000 | 0.004 | 0.000 | 0.000 | 0.000 | 0.004 |

| Hole: | 897D | 899B | | | | 899B | 899B | | 899B | |
|---|---|---|---|---|---|---|---|---|---|---|
| Core, section: | 24R-1 | 19R-3 | | | | 25R-2 | 29R-1 | | 30R-1 | |
| Interval (cm): | 0–5 | 9–14 | | | | 41–46 | 111–114 | | 83–86 | |
| Sample type: | V | B | ChV | V | V | B | MS | B | MS | MS |
| $SiO_2$ | 40.69 | 40.15 | 42.29 | 42.93 | 41.80 | 46.48 | 42.48 | 41.16 | 37.04 | 42.55 |
| $TiO_2$ | 0.02 | 0.02 | 0.01 | 0.02 | 0.02 | 0.03 | 0.06 | 0.04 | 0.02 | 0.06 |
| $Al_2O_3$ | 2.29 | 2.24 | 0.76 | 0.60 | 0.03 | 0.03 | 0.39 | 2.85 | 9.25 | 0.33 |
| $Cr_2O_3$ | 0.12 | 0.91 | 0.00 | 0.00 | 0.03 | 0.06 | 0.02 | 0.05 | 0.05 | 0.13 |
| FeO | 1.66 | 2.75 | 1.54 | 1.13 | 10.18 | 10.46 | 4.43 | 8.20 | 4.97 | 3.18 |
| MnO | 0.03 | 0.21 | 0.11 | 0.16 | 0.15 | 0.10 | 0.00 | 0.10 | 0.05 | 0.05 |
| NiO | 0.00 | 0.09 | 0.15 | 0.37 | 0.00 | 0.00 | 0.28 | 0.29 | 0.05 | 0.22 |
| MgO | 39.10 | 38.55 | 40.29 | 41.44 | 29.77 | 28.67 | 38.49 | 33.96 | 34.34 | 38.80 |
| CaO | 0.10 | 0.03 | 0.04 | 0.04 | 0.15 | 0.31 | 0.04 | 0.28 | 0.02 | 0.06 |
| $Na_2O$ | 0.05 | 0.05 | 0.02 | 0.26 | 0.74 | 0.08 | 0.00 | 0.01 | 0.05 | 0.04 |
| $K_2O$ | 0.02 | 0.00 | 0.00 | 0.10 | 0.09 | 0.01 | 0.02 | 0.00 | 0.11 | 0.00 |
| Total | 84.09 | 85.01 | 85.21 | 87.05 | 82.95 | 86.23 | 86.19 | 86.95 | 85.95 | 85.42 |
| Cl | 0.19 | 0.15 | 0.12 | 0.01 | 0.19 | | | | 0.03 | 0.12 |
| F | 0.00 | | | | | | | | | |
| (–O = F, Cl) | –0.09 | –0.07 | –0.06 | 0.00 | –0.08 | | | | –0.01 | –0.05 |
| Total | 84.20 | 85.10 | 85.28 | 87.05 | 83.05 | 86.23 | 86.19 | 86.95 | 85.97 | 85.48 |
| Si | 1.949 | 1.917 | 1.998 | 1.991 | 2.062 | 2.177 | 1.996 | 1.934 | 1.750 | 2.011 |
| Ti | 0.001 | 0.001 | 0.000 | 0.001 | 0.001 | 0.001 | 0.002 | 0.001 | 0.001 | 0.002 |
| Cr | 0.005 | 0.034 | 0.000 | 0.000 | 0.001 | 0.003 | 0.001 | 0.002 | 0.002 | 0.005 |
| $Fe^{3+}$ | 0.067 | 0.110 | 0.061 | 0.044 | 0.420 | 0.410 | 0.174 | 0.322 | 0.196 | 0.126 |
| Al | 0.129 | 0.126 | 0.042 | 0.033 | 0.002 | 0.002 | 0.022 | 0.158 | 0.515 | 0.018 |
| Mn | 0.001 | 0.008 | 0.004 | 0.006 | 0.006 | 0.004 | 0.000 | 0.004 | 0.002 | 0.002 |
| Ni | 0.000 | 0.003 | 0.006 | 0.014 | 0.000 | 0.000 | 0.010 | 0.011 | 0.002 | 0.008 |
| Mg | 2.791 | 2.743 | 2.836 | 2.865 | 2.189 | 2.001 | 2.696 | 2.378 | 2.418 | 2.734 |
| Ca | 0.005 | 0.002 | 0.002 | 0.002 | 0.008 | 0.016 | 0.002 | 0.014 | 0.001 | 0.003 |
| Na | 0.001 | 0.005 | 0.002 | 0.023 | 0.071 | 0.007 | 0.000 | 0.001 | 0.005 | 0.003 |
| K | 0.001 | 0.000 | 0.000 | 0.006 | 0.006 | 0.001 | 0.001 | 0.000 | 0.007 | 0.000 |
| Total | 4.949 | 4.949 | 4.951 | 4.984 | 4.764 | 4.620 | 4.904 | 4.824 | 4.898 | 4.913 |
| Cl | 0.000 | 0.012 | 0.010 | 0.001 | 0.016 | 0.000 | 0.000 | 0.000 | 0.002 | 0.009 |
| F | 0.000 | | | | | 0.000 | 0.000 | | 0.000 | 0.000 |

Notes: Formula unit calculated on 7 oxygen basis with Fe total as $Fe^{3+}$; V = vein, MS = mesh serpentine after olivine, B = bastite, ChV = chrysotile vein.

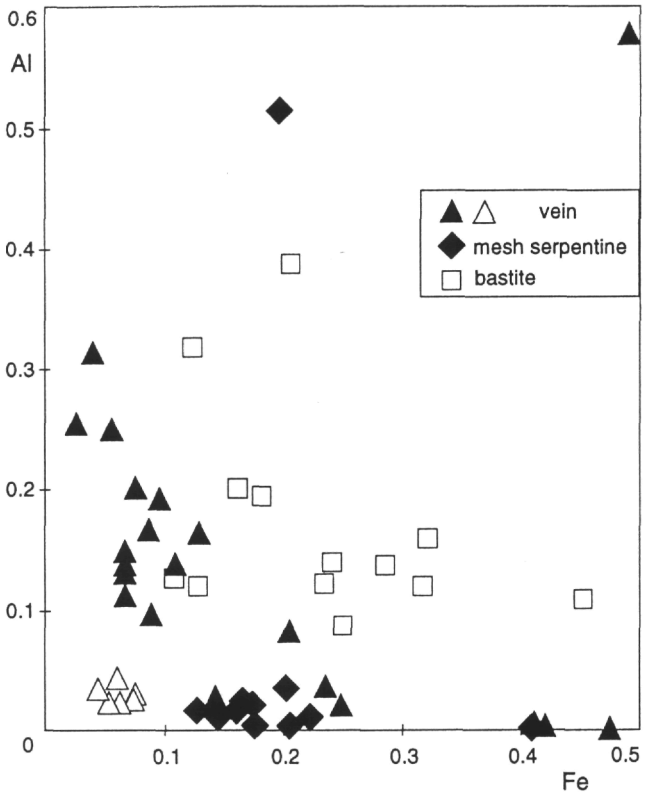


Figure 5. Al vs. Fe (atom per formula unit) diagram discriminating the serpentine according to their different setting. Open triangles = chrysotile and low-Al, low-Fe pseudomorphs of chrysotile; solid triangles = lizardite.

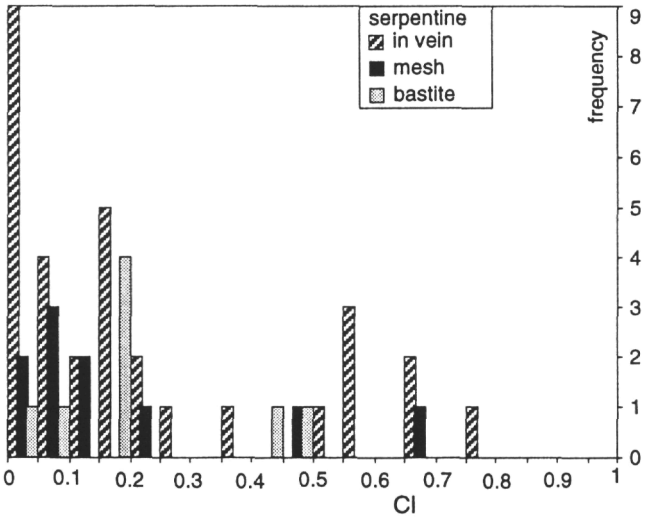


Figure 6. Histogram of the chlorine content (wt%) in serpentine, according to their situation.

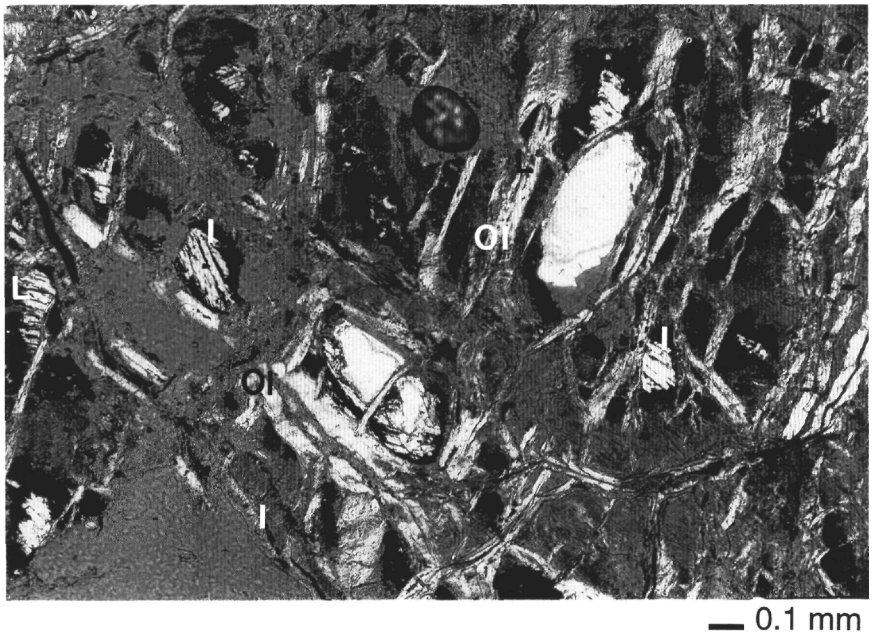


Figure 7. Photomicrograph of the dunite Sample 149-897C-70R-1, 6-9 cm, showing olivine (Ol) remnants and iowaite (I) inside the mesh network of lizardite (L).

**Table 5. Selected microprobe analyses of iowaite, brucite, and pink "mineral" (mixture of serpentine, iowaite, and altered spinel; see text).**

| Hole: | 897C | | | 897D | | | |
|---|---|---|---|---|---|---|---|
| Core, section: | 70R-1 | | | 17R-6 | | | |
| Interval (cm): | 6–9 | | | 5–10 | | | |
| Sample type: | Iowaite | | Brucite | Pink "mineral" | | | |
| $SiO_2$ | 0.47 | 0.20 | 0.00 | 12.16 | 16.72 | 19.10 | 28.00 |
| $TiO_2$ | 0.00 | 0.00 | 0.00 | 0.00 | 0.00 | 0.00 | 0.00 |
| $Al_2O_3$ | 0.93 | 0.94 | 0.00 | 0.43 | 0.36 | 0.57 | 0.70 |
| $Cr_2O_3$ | 0.00 | 0.00 | 0.04 | 13.63 | 11.96 | 14.30 | 6.95 |
| FeO | 18.77 | 18.11 | 0.02 | 2.96 | 2.08 | 1.87 | 2.88 |
| MnO | 0.05 | 0.00 | 0.09 | 0.04 | 0.00 | 0.06 | 0.15 |
| NiO | 0.00 | 0.00 | 0.00 | 0.19 | 0.14 | 0.07 | 0.27 |
| MgO | 43.41 | 42.93 | 68.41 | 38.03 | 35.75 | 37.82 | 36.33 |
| CaO | 0.02 | 0.00 | 0.04 | 0.09 | 0.13 | 0.08 | 0.08 |
| $Na_2O$ | 0.01 | 0.04 | 0.01 | 0.04 | 0.04 | 0.00 | 0.00 |
| $K_2O$ | 0.01 | 0.00 | 0.00 | 0.00 | 0.01 | 0.00 | 0.00 |
| Cl | 3.40 | 4.88 | 0.01 | 1.36 | 2.12 | 2.14 | 0.89 |
| F | 0.00 | 0.00 | 0.00 | 0.06 | 0.00 | 0.00 | 0.00 |
| Total | 67.07 | 67.08 | 68.61 | 68.98 | 69.31 | 76.01 | 76.22 |
| (–0 = F, Cl) | –1.536 | –2.2 | –0 | –0.67 | 0.96 | –0.97 | –0.4 |
| Total | 65.529 | 64.881 | 68.611 | 68.316 | 68.351 | 75.040 | 75.823 |

**Table 6. $^{18}O/^{16}O$ and $^{13}C/^{12}C$ analyses of serpentines, magnetites, and calcites from Leg 149.**

| Core, section, interval (cm) | Piece number | Serpentine $\delta^{18}O$ (‰) | Magnetite $\delta^{18}O$ (‰) | Calcite $\delta^{18}O$ (‰) | Calcite $\delta^{13}C$ (‰) | Calcite [$CaCO_3$] (wt%) |
|---|---|---|---|---|---|---|
| 149-897C- | | | | | | |
| 65R-1, 48–52 | 3B | 10.9 | | 29.6 | 1.0 | 18.6 |
| 72R-1, 40–47 | 1E | 9.6 | –1.4 | | | |
| 149-897D- | | | | | | |
| 16R-2, 35–42 | 1C | 3.8 | | 29.7 | 2.4 | 85.0 |
| 19R-1, 85–88 | 8E | 11.8 | | | | |
| 19R-4, 28–35 | 1A | 11.3 | | | | |
| 19R-5, 62–69 | 3A | 8.8 | | | | |
| 20R-2, 115–120 | 4C | 12.2 | | | | |
| 23R-1, 62–68 | 5C | 10.5 | –2.0 | | | |
| 24R-1, 0–5 | 1 | 9.4 | | | | |
| 149-899B- | | | | | | |
| 18R-2, 18–23 | 1A | | | 31.1 | 1.1 | 21.5 |
| 19R-2, 0–5 | 1 | | | 31.1 | 0.0 | 87.1 |
| 20R-2, 100–107 | 5D | | | 30.7 | –0.6 | 57.7 |
| 23R-3, 121–125 | 21 | | | 30.6 | –0.7 | 38.0 |
| 24R-3, 87–92 | 12A | | | 30.9 | 0.5 | 83.4 |
| 28R-1, 118–125 | 13B | | | 30.6 | –0.2 | 88.2 |